Molecular dynamics simulation of CO2 hydrates: Prediction of three phase coexistence line

J. M. Míguez, M. M. Conde, J.-P. Torré, F. J. Blas, M. M. Piñeiro, and C. Vega

Citation: The Journal of Chemical Physics **142**, 124505 (2015); doi: 10.1063/1.4916119
View online: http://dx.doi.org/10.1063/1.4916119
View Table of Contents: http://scitation.aip.org/content/aip/journal/jcp/142/12?ver=pdfcov
Published by the AIP Publishing

Molecular dynamics simulation of CO_2 hydrates: Prediction of three phase coexistence line

J. M. Míguez,[1] M. M. Conde,[1] J.-P. Torré,[1] F. J. Blas,[2] M. M. Piñeiro,[3,a)] and C. Vega[4]
[1]*Laboratoire des Fluides Complexes et leurs Réservoirs, UMR 5150, Université de Pau et des Pays de l'Adour, B. P. 1155, Pau-Cedex 64013, France*
[2]*Departamento de Física Aplicada, Facultad de Ciencias Experimentales, and Centro de Física Teórica y Matemática FIMAT, Universidad de Huelva, 21071 Huelva, Spain*
[3]*Departamento de Física Aplicada, Facultade de Ciencias, Universidade de Vigo, E36310 Vigo, Spain*
[4]*Departamento de Química-Física I, Facultad de Ciencias Químicas, Universidad Complutense de Madrid, E28040 Madrid, Spain*

(Received 22 December 2014; accepted 11 March 2015; published online 27 March 2015)

The three phase equilibrium line (hydrate-liquid water-liquid carbon dioxide) has been estimated for the water + carbon dioxide binary mixture using molecular dynamics simulation and the direct coexistence technique. Both molecules have been represented using rigid nonpolarizable models. TIP4P/2005 and TIP4P/Ice were used for the case of water, while carbon dioxide was considered as a three center linear molecule with the parameterizations of MSM, EPM2, TraPPE, and ZD. The influence of the initial guest occupancy fraction on the hydrate stability has been analyzed first in order to determine the optimal starting configuration for the simulations, paying attention to the influence of the two different cells existing in the *sI* hydrate structure. The three phase coexistence temperature was then determined for a pressure range from 2 to 500 MPa. The qualitative shape of the equilibrium curve estimated is correct, including the high pressure temperature maximum that determines the hydrate re-entrant behaviour. However, in order to obtain quantitative agreement with experimental results, a positive deviation from the classical Lorentz-Berthelot combining rules must be considered. © *2015 AIP Publishing LLC.* [http://dx.doi.org/10.1063/1.4916119]

I. INTRODUCTION

Gas hydrates are nonstoichiometric inclusion solid compounds, where small guest molecules are enclathrated in the voids left by a periodic network of water molecules, which may adopt at least three different crystalline structures,[1,2] denoted as *sI*,[3] *sII*,[4] and *sH*.[5] Research on gas hydrates has been motivated to a great extent lately by the huge amount of methane that has been identified in hydrate deposits, either in the sea floor or in permafrost frozen substrates.[6,7] This fact makes hydrates a key future energetic source, whose exploitation represents a technical challenge of first magnitude.[8–12] Besides this primary motivation, there are other remarkably relevant scientific and practical interests of hydrates,[13] as, for example, the possibility to capture[14,15] and store[16] carbon dioxide, which place hydrates at the center of environmental concerns regarding atmospheric greenhouse gases.

In this scenario, hydrates have become a scientific topic that concentrates huge global research efforts, from diverse perspectives and concerning many scientific disciplines. From a theoretical modeling point of view, Molecular Simulation (MS, hereafter for brevity) has been intensively applied, as detailed recently in the excellent reviews by Sum *et al.*[17] and Barnes and Sum.[18] Many of the published studies in this area are concerned with hydrate nucleation, metastability, and growth. The reason for this is that MS offers insight into atomic level phenomena that are not observable from an experimental point of view, due to the time (nanoseconds) and distance (nanometers) scales involved. This provides unique and invaluable information about the underlying physicochemical principles governing hydrate behaviour. The simulation of dynamic phenomena, whose driving principles and mechanisms are not fully understood yet, has advanced in parallel with the increase in computing ability, and, for instance, the first direct simulation of spontaneous nucleation and growth of methane hydrate was published only very recently by Walsh *et al.*[19] In this field, MS has acquired for these reasons a crucial role and has become a extensively used exploration tool.

Concerning the MS analysis of hydrates thermophysical properties and phase equilibria, despite the practical importance of these goals, the number of related studies is reduced yet, due to the large size and complexity of the molecular systems that need to be considered, which imposes a practical limit for the remarkably large computing times required. Most published works have focused so far on CH_4 hydrates. Nevertheless, there is an increasing interest on exploring the practical feasibility of replacing CH_4 by CO_2 in existing hydrates deposits.[20] The global concern about greenhouse gases emissions control is undoubtedly one of the most urgent environmental threatens to be faced in the immediate future, and so, research on CO_2 hydrates characterization is receiving increasing attention nowadays. Just to cite a few related contributions, Yezdimer *et al.*[21] performed free energy calculations using MS stating the thermodynamic feasibility

a)Electronic mail: mmpineiro@uvigo.es

of this replacement process, and Dornan *et al.*[22] followed a similar approach reaching similar conclusions. Bai *et al.*[23,24] also studied the replacement phenomenon, stating that the CO_2 hydrate nucleates near the three phase contact line. Tung *et al.*[25,26] also concentrated in the same process, concluding that the replacement may occur without melting of the original CH_4 hydrate. Sarupria and Debenedetti[27] analyzed the CO_2 hydrate dissociation using molecular dynamics (MD) and rigid nonpolarizable molecular models, similar to the ones selected in this work. Concerning thermophysical properties and phase equilibria, Chialvo *et al.*[28] reported MD results for both CH_4 and CO_2 type *sI* hydrates. Sun and Duan[29] studied CH_4 and CO_2 hydrates phase equilibria using MD with Lennard Jones (LJ) interaction potentials whose parameters were tuned from *ab initio* calculation results. There is an important body of quantum *ab initio* calculation studies about hydrates. This alternative theoretical approach provides crucial information on many microscopic energetic and structural features not accessible to MS techniques, representing an alternative and complementary calculation level (see, for instance, Vidal-Vidal *et al.*[30] and references therein). As another combination of both approaches, recently Velaga and Anderson[31] used preliminary quantum calculations to parameterize an intermolecular model and describe CO_2 hydrate phase equilibria. The influence of nuclear quantum effects on hydrate structures has been also considered by Conde *et al.*[32]

Nevertheless, CO_2 hydrates phase equilibrium calculations using MS are scarce. An important element in hydrates global phase diagram, in a *PT* projection, is the three phase line. Along this line, the hydrate coexists with two fluid phases, one rich in H_2O and the other rich in the hydrate former guest molecule. At a certain pressure P, there is a three phase equilibrium temperature value T_3 (the subscript 3 standing for three phase), representing the upper limit for obtaining the hydrate from the fluid phases. Wierzchowski and Monson[33,34] determined this equilibrium for different hydrates using free energy calculations and Monte Carlo simulations. Conde and Vega[35,36] used the direct coexistence technique and molecular dynamics to estimate CH_4 hydrate coexistence. In these works, the quantitative performance of different rigid nonpolarizable H_2O molecular models was compared, finding that the consideration of positive deviation from the ideal Lorentz-Berthelot combining rules represented an effective solution to account for molecular polarizability, yielding a remarkable representation of experimental coexistence results. Very recently, Michalis *et al.*[37] applied the same MD direct coexistence technique to estimate three phase equilibria for CH_4 type *sI* hydrates.

The objective of this work is the estimation of the three phase equilibrium line (hydrate-liquid CO_2-liquid H_2O) for the CO_2-H_2O binary mixture using molecular dynamics. The technique used will be that proposed by Conde and Vega.[35,36] Provided that the superiority of H_2O TIP4P/2005 and TIP4P/Ice molecular models in the hydrate phase equilibria estimation has been well established (see, e.g., Refs. 38–40 apart from those already cited), these two models will be used here, and their performance will be compared. For the case of CO_2, different three site rigid linear models will be evaluated, with also a simplified single sphere Lennard-Jones version for the sake of comparison, evaluating the influence of the model in the phase equilibria estimation. The occupancy rate of the guest molecules in the structure hydrate will be studied as well, because this factor has been pointed out to affect the structure stability. So, different initial occupancy rates for the two building cells existing in this hydrate will be considered. Finally, the quantitative correspondence of the three phase line estimation with experimental data will be discussed, together with the adequacy of considering nonideal combining rules to describe the H_2O-CO_2 interaction.

II. MOLECULAR MODELS AND SIMULATION DETAILS

The type of hydrate is mainly determined by the size of the guest molecules which occupy the cavities or cages of these structures. Small molecules, such as CH_4, C_2H_6, or CO_2, adopt *sI* hydrate structure, which is a cubic structure with the space group $Pm\bar{3}n$ and a lattice parameter of about 12 Å. The unit cell of structure *sI* contains six tetradecahedrons (denoted hereafter as T for simplicity), $5^{12}6^2$, and two pentagonal dodecahedron (denoted as D) 5^{12} cavities. Therefore, the unit cell is built by 46 H_2O molecules forming eight cavities (six large T and two small D cavities). D cages are nearly spherical with an average radius of about 3.95 Å, while T cages present an average radius of about 4.33 Å.[1] As starting point for the calculations presented in this work, we have generated the unit cell of structure *sI* from the crystallographic coordinates provided by Yousuf *et al.*[41]

Then, the initial CO_2 hydrate configuration was obtained by replicating this unit cell twice in each spacial direction, $(2 \times 2 \times 2)$, using a total of 368 water molecules which leave 64 cavities. It is well-known that hydrates present proton disorder, and thus hydrogen atoms were placed using the algorithm proposed by Buch *et al.*,[42] with the aim to generate solid configurations satisfying the Bernal-Fowler rules,[43] with zero (or at least negligible) dipole moment. Fig. 1 shows X-Z, X-Y, and Y-Z projections of this initial hydrate configuration. In the case of CO_2 as guest particle, occupancy was calculated as the percent of cages filled per unit cell. The simulations were initialized starting from five different CO_2 occupancy states, as detailed in Table I. The occupancy ratios vary from 100% (all cages filled) to 37.5% (only half of T cages occupied). When the occupancy of a certain type of cages (T or D) is not 100%, the occupied cages are selected randomly. This study allowed exploring the effect of the distribution of guest molecules in the different cage types on hydrate stability, while determining the three phase coexistence line (hydrate-H_2O-CO_2) through the mechanisms of hydrate dissociation and crystallization.

The initial simulation box was generated by further adding two fluid phases of H_2O and CO_2, respectively, along the x-axis of the original box containing the crystal structure. Hence, the initial configuration was formed by a slab of CO_2 fluid phase, with a slab of CO_2 hydrate at one side and a slab of H_2O liquid in the other side (see Fig. 2). The fluid phase of H_2O contained 368 molecules and that of CO_2 contained 192 molecules in all cases. The length of each fluid slab is equal to the length of the

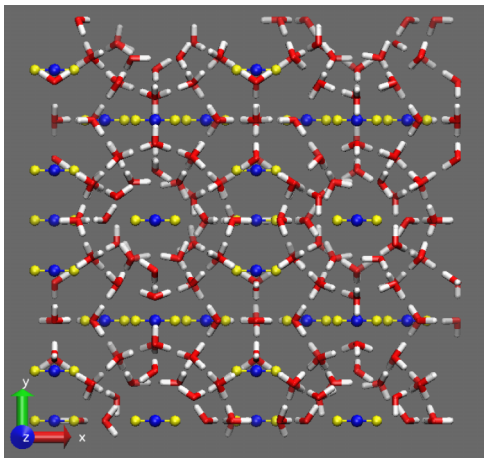

(a)

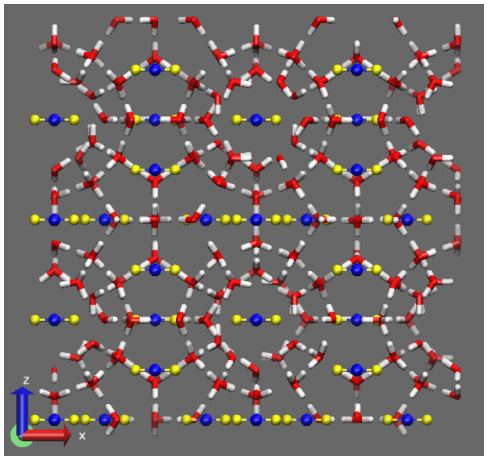

(b)

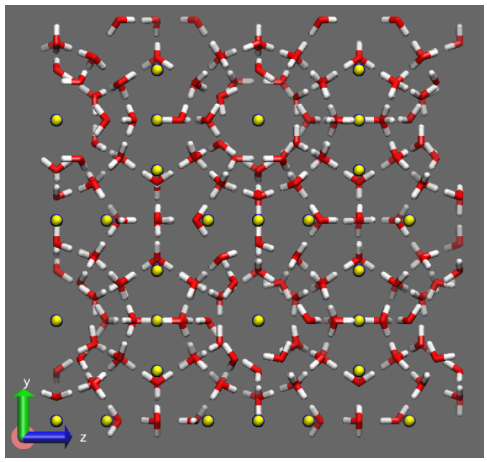

(c)

FIG. 1. Projections of the initial CO_2 hydrate configuration used: (a) x-y view, (b) x-z view, and (c) z-y view. This configuration is composed by 368 bonded H_2O (O-red and H-white) molecules and 64 CO_2 (C-blue and O-yellow) molecules occupying all the cages.

hydrate structure. The typical lengths of the simulation box for the initial configuration were $L_y = L_z = 24$ Å and $L_x = 72$ Å. The interfaces between the three phases are perpendicular to the x-axis. The initial spacial arrangement was selected to have each phase in contact with the other two, enabling the study of hydrate crystallization and dissociation at different pressure and temperature conditions.

TABLE I. Cage occupancy for the initial CO_2 hydrate structure (θ_T: occupancy of T cages; θ_D: occupancy of D cages).

Case	Occupancy (%)	θ_T (%)	θ_D (%)
1	100	100	100
2	87.5	100	50
3	75	100	0
4	50	50	50
5	37.5	50	0

All MD simulations were carried out in the isothermal-isobaric NPT ensemble using GROMACS (version 4.6.1).[44] The isobars of 2, 3, 5, 6, 10, 20, 40, 100, 200, 300, 400, and 500 MPa were explored. Constant temperature and pressure were kept using a Nosé-Hoover[45,46] thermostat and a Parrinello-Rahman[47,48] barostat with a relaxation time of 2 ps. The three different sides of the simulation box were allowed to fluctuate independently. This enables changes in the shape of the solid region and avoids the appearance of stress forces on it. The usual complete periodic boundary conditions and minimum image convention were respected. The time-step used was 2 fs, and the typical length of the runs varied between 80 ns (dissociation) and 400 ns (crystallization). Intermolecular interactions were calculated as a sum of two contributions, LJ pairwise interactions, which were truncated at 9 Å, and electrostatic interactions, dealt with the Ewald sums method. The real part of the Coulombic potential was truncated also at 9 Å and the Fourier term of the Ewald sums was evaluated using the Particle Mesh Ewald (PME) method.[49] The width of the mesh was 1 Å with a relative tolerance of 10^{-3} Å.

H_2O was modelled using the well-known rigid non-polarizable TIP4P[50] molecular geometry: four interacting centres, with the oxygen atom O as the only LJ interaction site, a point electric charge (M-site) located along the H-O-H angle bisector, and two hydrogen atoms H, which are represented by point electric charges. Recently, Conde and Vega[35,36] estimated the three phase hydrate-H_2O-CH_4 coexisting line using different water potential models (SPC,[51,52] SPC/E,[53] TIP4P,[50] TIP4P/2005,[54] and TIP4P/Ice[55]). A comparison with experimental results revealed the limitations of these models, and also showed that TIP4P/2005 and TIP4P/Ice are the most accurate among them to study CH_4 hydrate phase

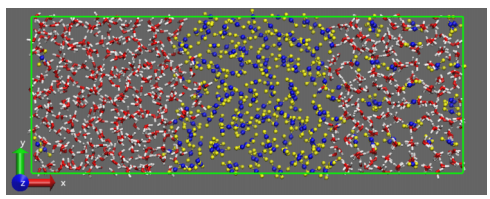

FIG. 2. Snapshot of the initial configuration formed by a slab of liquid CO_2 surrounded by a slab of CO_2 hydrate and a slab of liquid H_2O molecules. H_2O molecules are plotted in red and white and CO_2 molecules in blue and yellow. The initial box dimensions are $x = 72$ Å, $y = 24$ Å, and $z = 24$ Å.

TABLE II. Lennard-Jones potential well depth ϵ and size σ, partial charges q, and geometry, of the H_2O and CO_2 models used.

Atom	ϵ/κ_B (K)	σ (Å)	$q(e)$	Geometry
TIP4P/2005 H_2O				
O	93.20	3.1589	0.0	O-H: 0.9572 Å
H	0.0	0.0	0.5564	O-M: 0.1546 Å
M	0.0	0.0	−1.1128	H-O-H: 104.52°
TIP4P/Ice H_2O				
O	106.1	3.1668	0.0	O-H: 0.9572 Å
H	0.0	0.0	0.5897	O-M: 0.1577 Å
M	0.0	0.0	−1.1794	H-O-H: 104.5°
MSM CO_2				
C	29.0	2.785	0.5957	C-O: 1.16 Å
O	83.1	3.014	−0.297 85	O-C-O: 180°
EPM2 CO_2				
C	28.129	2.757	0.6512	C-O: 1.149 Å
O	80.507	3.033	−0.3256	O-C-O: 180°
TraPPE CO_2				
C	27.0	2.80	0.70	C-O: 1.16 Å
O	79.0	3.05	−0.35	O-C-O: 180°
ZD CO_2				
C	28.845	2.7918	0.5888	C-O: 1.163 Å
O	82.656	3.0	−0.2944	O-C-O: 180°

equilibria. Assuming these conclusions, we have also selected the TIP4P/2005 and TIP4P/Ice parametrizations to describe H_2O in this work.

In the case of CO_2, the most popular model in the category of rigid non-polarizable is a linear chain with three interacting sites, representing the C and O atoms, and each of them consisting on a combination of a LJ site plus an electric point charge. Among the available parametrizations for this structure, in this study, the original version of MSM,[56–58] EPM2[59] (a variation of the original EPM, standing for Elementary Physical Model), TraPPE[60] (Transferable Potentials for Phase Equilibria), and ZD (Zhang and Duan[61]) models were tested. Table II summarizes the characteristic parameters for all the molecular models considered.

The LJ H_2O-CO_2 interaction was calculated using the crossed interaction parameters given by the Lorentz-Berthelot combining rules:[62]

$$\epsilon_{ij} = \chi(\epsilon_{ii} \cdot \epsilon_{jj})^{1/2}, \quad (1)$$

$$\sigma_{ij} = \frac{1}{2}\left(\sigma_{ii} + \sigma_{jj}\right), \quad (2)$$

where i and j stand for each of the species, and the ideal combination rule is obtained if $\chi = 1$.

Conde and Vega[35,36] recommended positive deviations from the energetic Lorentz-Berthelot combination rules to adequately describe the three phase coexistence line of CH_4 hydrates using TIP4P/2005 model in combination with a LJ center for CH_4, which means that $\chi \geq 1$ is considered in Eq. (1). In this work, the ideal case (i.e., $\chi = 1$) has been used as a general rule, except for the case of the combination of TIP4P/Ice H_2O and TraPPE CO_2, where a value of $\chi = 1.13$ has been also tested, as it will be discussed later.

III. RESULTS

A. Specific-cage occupancy of the initial CO_2 hydrate configuration

In the last few years, initial hydrate occupancy has represented an important issue studied by several authors from MS point of view.[27,63–67] English *et al.*[63] showed that the CH_4 hydrate decomposition rates computed using MD do not depend strongly on the initial cage occupancy for starting values in the range of 80%-100% occupancy. Later, Myshakin *et al.*[64] observed, in contrast with the precedent results, that the presence of empty cages substantially destabilizes the CH_4 hydrate lattice and speeds up around 30% hydrate decomposition. Sarupria *et al.*[27] performed a detailed work about CO_2 hydrate dissociation using initial occupancy values from 100% to 87% and found no evidence of the influence of hydrate occupancy on melting point estimation for a hydrate-H_2O binary system. However, they reported that the kinetics of hydrate dissociation is sensitive to cage-specific occupancy and not only to overall occupancy. Then, there are discrepancies between different authors concerning the influence of this factor, and an agreement seems to exist[27,35] on the fact that this issue should be analyzed in further detail.

Following this discussion, we have studied the cage-specific occupancy dependence on the initial hydrate phase to predict the three phase coexistence temperature T_3 (hydrate-liquid H_2O-liquid CO_2) analyzing crystallization and dissociation runs at 40 MPa and temperatures from 260 to 280 K. We have investigated five different initial CO_2 hydrate compositions: 100%, 87.5%, 75%, 50%, and 37.5%. These particular values were selected with the aim to try to elucidate the role of T and D cell occupancy values (listed

TABLE III. Number of molecules in the different phases for every case studied. x_{CO_2} is the overall CO_2 mole fraction in the system.

Case	Hydrate phase	*Fluid phase* 1/*fluid phase* 2	x_{CO_2}
1	368 H_2O/64 CO_2	368 H_2O/192 CO_2	0.258
2	368 H_2O/56 CO_2	368 H_2O/192 CO_2	0.252
3	368 H_2O/48 CO_2	368 H_2O/192 CO_2	0.246
4	368 H_2O/32 CO_2	368 H_2O/192 CO_2	0.233
5	368 H_2O/24 CO_2	368 H_2O/192 CO_2	0.227

in Table I) on hydrate stability. The number of molecules of each molecule in the different phases present and the overall CO_2 mole fraction have been listed in Table III. For the purpose of this work, Fig. 3 shows the *PT* experimental phase diagram of CO_2 hydrate.[1] As can be seen, the relevant region of the hydrate phase diagram comprises two regions separated by a three phase coexistence line (hydrate-liquid H_2O-liquid/vapour CO_2). At 40 MPa, CO_2 hydrate is in equilibrium with liquid CO_2 until a temperature of 286.2 K. Beyond this three phase coexistence temperature T_3, the hydrate dissociates and the system presents liquid equilibria (LLE) between H_2O and CO_2. Therefore, we can estimate T_3 as the arithmetic average of the highest temperature at which the CO_2 hydrate crystallizes and the lowest temperature at which the hydrate dissociates.[35,36]

Fig. 4 shows the potential energy fluctuations as a function of time for the three phase initial system composed by liquid H_2O, liquid CO_2, and CO_2 hydrate (see Figure 2). The potential energy evolution of the system for different cases of CO_2 hydrate initial composition has been illustrated. Simulations were performed using TIP4P/Ice H_2O and TraPPE[60] CO_2 at this selected 40 MPa value.

In the cases of 100%, 87.5%, and 75% initial hydrate slab occupancy, it is possible to distinguish two different behaviours of the potential energy time evolution. At the higher temperature values tested, energy increases consistently to reach a final plateau indicating that the hydrate slab has completely melt, resulting in an equilibrium state of two fluid phases. This is the case for the temperatures from 272 K to 285 K. The dissociation process speeds up when temperature increases and the energy behaviour is similar regardless of the initial hydrate occupancy value. The steep increase in the energy immediately prior to the final plateau corresponds to the melting of the last layer of the hydrate. This steep increase is common to the cases of CH_4[35] and CO_2[27] hydrates. Figs. 5(a) and 5(c) show a snapshot of the final LLE state and an averaged density profile of the system along the *x*-axis. However, at low temperatures, the potential energy decreases to reach a final plateau after 250 ns, indicating complete crystallization of liquid H_2O in presence of CO_2 leading to an equilibrium state of two phases (hydrate-liquid CO_2). This is the case for the temperatures from 260 to 270 K. The potential energy evolution is similar again for all initial hydrate slab occupancies. Figs. 5(b) and 5(d) show a snapshot of the final hydrate-liquid CO_2 equilibrium state and an averaged density profile of the system along the *x*-axis.

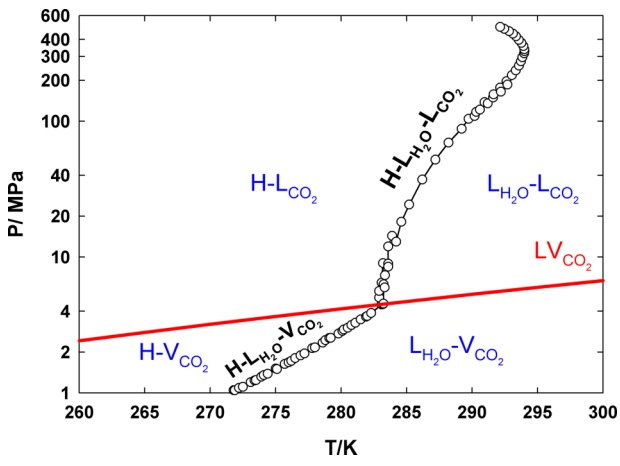

FIG. 3. Experimental *PT* projection of the three-phase coexistence line of CO_2 hydrates: (black open circles) experimental data and (red line) experimental CO_2 vapor pressure.

In our simulations, the growth of the CO_2 hydrate has occurred layer by layer beginning at the interface of liquid H_2O and hydrate slab (see Figure 6). CO_2 molecules diffuse through the slab of liquid H_2O until they reach the hydrate surface. Then, H_2O liquid molecules start to accommodate around these CO_2 molecules to grow the hydrate phase, a process limited by the transport of CO_2 to the hydrate/H_2O fluid interface. The occupancy rate of these newly grown hydrate layers has not been quantified in detail in this work but an inspection of some on the configurations obtained reveals rates very close to those of the already existing hydrate layers. As it is well known, the solubility of CO_2 in liquid H_2O is very low at these conditions,[68] and these simulations are quite expensive from a computational point of view. In fact, the time estimated to obtain complete crystallization runs was around 400 ns. The fast growth of the CO_2 hydrate, which occurs once a supersaturated solution of CO_2 in liquid water is formed, is not observed is our simulations. In this work, we have not observed the formation of bubbles of CO_2 within the H_2O phase. In previous works,[19,35,69–72] formation of bubbles of CH_4 dissolving into the aqueous phase was observed under certain conditions, leading to the formation of supersaturated solutions. Further work is needed to analyze the origin of the difference between CO_2 and CH_4. If nanobubles are relevant to describe the memory effect, then CO_2 and CH_4 may have different behaviour in that respect. Further work is needed to analyze these aspects in more detail.

In summary, Figures 4(a)–4(c) show the same energy behaviour for three different initial hydrate cage occupancies. In these cases, CO_2 hydrate dissociates at 40 MPa above 272 K and crystallizes below 270 K. According to the previous criterion, the three phase coexistence temperature for TIP4P/Ice-H_2O and TraPPE-CO_2 is $T_3 = 271 \pm 2$ K at this pressure. We have obtained the same T_3 for the three different initial composition of CO_2 hydrate slab cited. At the same time, we have studied the crystallization and dissociation process of the system analyzing the potential energy evolution. The common feature of the configurations with initial 100%, 87.5%, and 75% occupancy is that all T cages are initially occupied.

Contrarily to these observations, initial hydrate compositions of 50% and 37.5% cannot predict hydrate-liquid CO_2 phase state equilibrium because hydrate slab dissociates at all

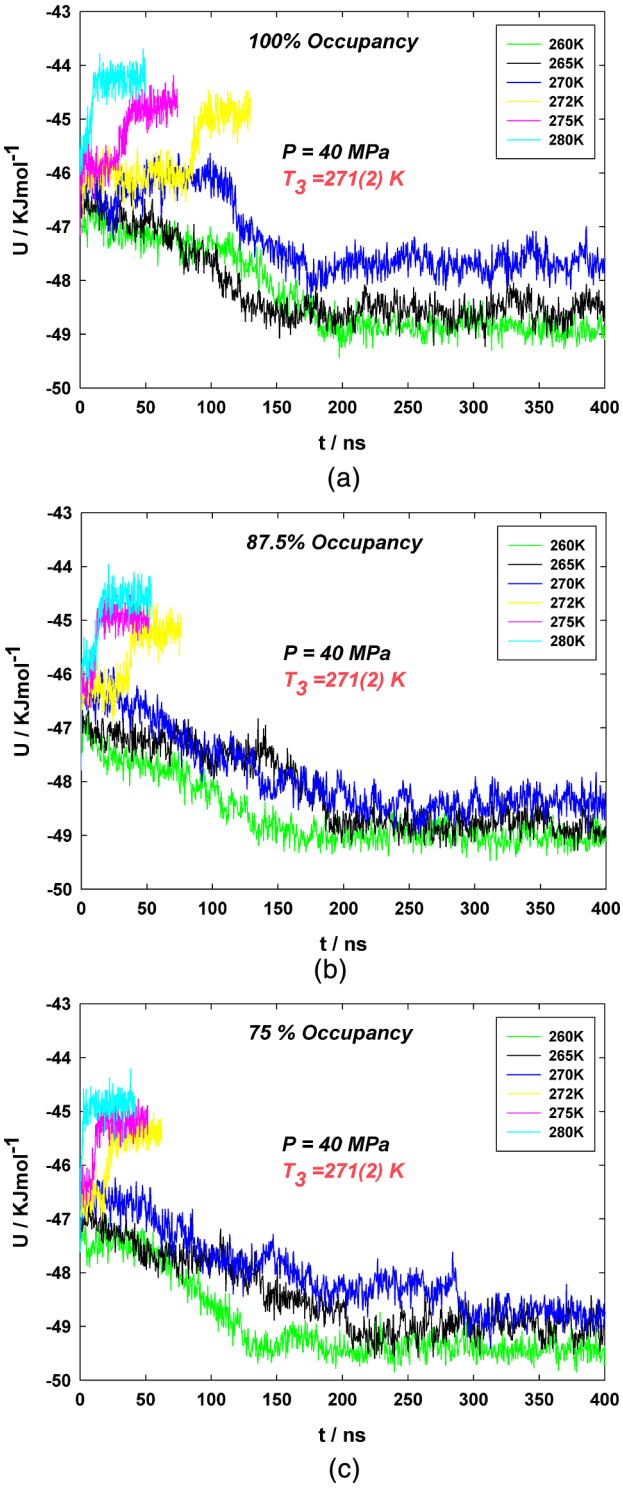

FIG. 4. Evolution of the potential energy of the three phase initial configuration (hydrate-H_2O-CO_2) as a function of time for the NPT simulations at 40 MPa and temperatures from 260 to 280 K. TIP4P/Ice H_2O and TraPPE CO_2 were used. The cage occupancy of the initial hydrate configuration was (a) case 1%-100%, (b) case 2%-87.5%, and (c) case 3%-75%.

temperatures. This means that the estimations of the model selected are in accordance with experimental X-ray diffraction results, which indicate that CO_2 hydrates with empty T cages and filled D cages cannot be formed (case 4), and there is a minimum threshold for T cage occupancy to ensure hydrate stability (case 5). In this sense, the estimations obtained for the combination of molecular models selected are physically sound. These initial hydrate configurations did not allow the calculation of three phase coexistence temperature T_3 at 40 MPa. These calculations state that the presence of empty T cavities destabilizes the hydrate slab, in accordance with the conclusions of Sarupria *et al.*[27] The presence of empty or occupied D cages does not change the evolution of the system, but it is necessary to remark that the number of D cavities is four times smaller.

B. Calculation of three phase coexistence line of CO_2 hydrate

Now, we present the prediction of the three phase coexistence line (hydrate-liquid H_2O-liquid CO_2) using several molecular models for both substances. For all simulations, we have used the same initial configuration, composed by liquid H_2O, liquid CO_2, and hydrate. In Sec. III A, we have demonstrated that the evolution of the initial system does not change for three different initial cage occupancy values for the hydrate slab (100%, 87.5%, and 75%). The three initial hydrate compositions lead to the same prediction of three phase coexistence temperature, T_3, at 40 MPa. Furthermore, experimental results suggest an occupancy range of 80%–100%[29,73,74] in the case of CO_2 hydrates. In particular, experimental estimations show that CO_2 occupies above 95% of T cages, while vacancies are mainly observed in D cavities. For these reasons, an initial value of 87.5% hydrate slab occupancy was selected to perform this part of the study, as given in line 2 of Table I.

We have performed NPT MD simulations along different isobars of 2, 3, 6, 10, 20, 40, 100, 200, 300, 400, and 500 MPa. All points of the three phase coexistence line were calculated using the same methodology. At each fixed pressure, the evolution of the system was analyzed at different temperatures with a 5 K step. When different final equilibrium states (liquid CO_2-liquid H_2O or hydrate-liquid CO_2) were identified for two consecutive runs along one isobar, one additional simulation was performed at an intermediate temperature. A minimum of five simulations have been analyzed to determine each T_3 value (see Fig. 4). Thus, the uncertainty on the calculation of T_3 can be estimated to be lower than 2 K. Although we have only estimated this uncertainty by direct coexistence simulations in the NPT ensemble, the system size ($\approx$1000 molecules) minimizes the impact of stochasticity in the determination of the coexistence point.[75] Results for T_3 were obtained using two different H_2O models, namely, TIP4P/2005[54] and TIP4P/Ice[55] with CO_2 described by five different models: four different versions of the rigid linear three site model (MSM,[56–58] TraPPE,[60] EPM2,[59] ZD[61]). The cross interactions were described by Lorentz-Berthelot rules without modifications at this stage.

Fig. 7 shows the prediction of the three phase coexistence line obtained for TIP4P/2005 and TIP4P/Ice H_2O and TraPPE model of CO_2. As shown, only estimations above the saturation curve of CO_2 have been obtained, because at low pressures, the time necessary to determine T_3 is out of computer possibilities (i.e., the solubility of CO_2 decreases with P, and the dynamics of growth of the hydrate becomes very

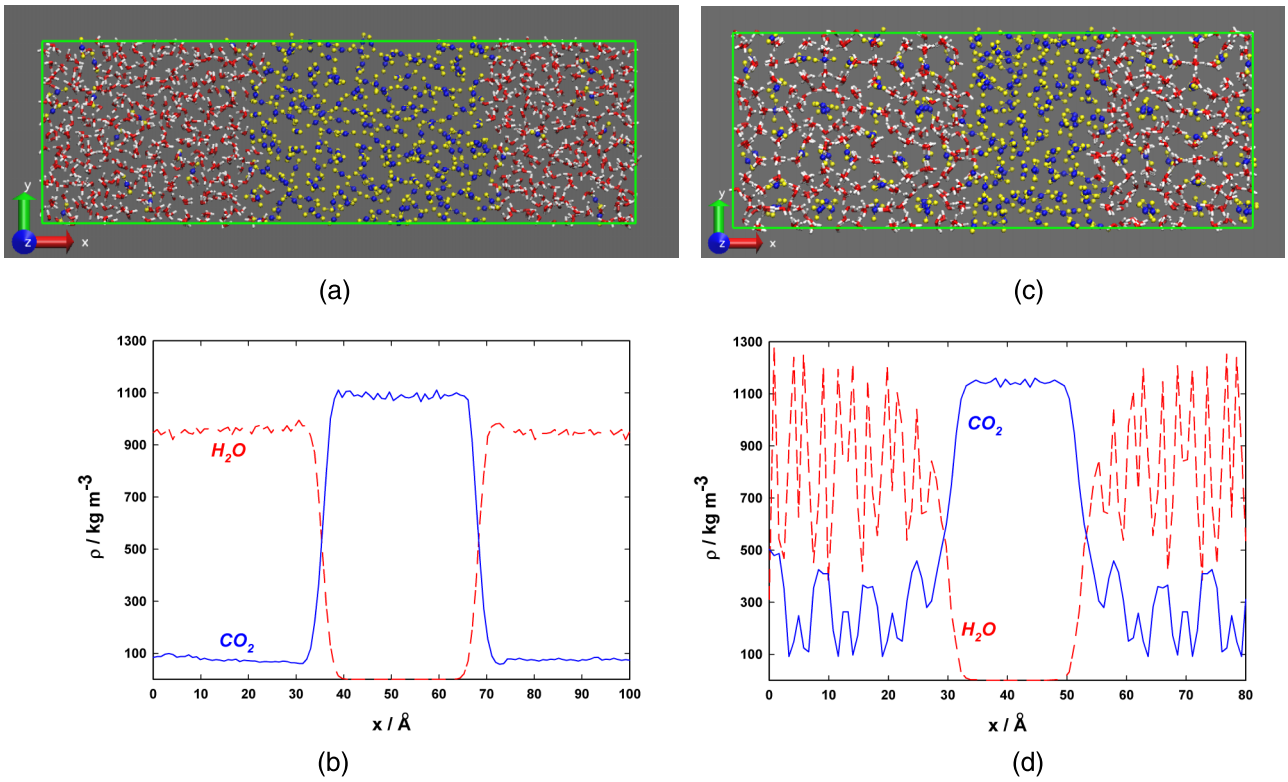

FIG. 5. Snapshots of the final states with their corresponding density profiles along the x-axis at 100 MPa. (a) and (b) Liquid H_2O (TIP4P-Ice) and liquid CO_2 (TraPPE) at 275 K; (c) and (d) hydrate and liquid CO_2 at 270 K. H_2O molecules are plotted in red and white and CO_2 molecules in blue and yellow.

slow under these conditions). Results of T_3 for TIP4P/Ice combined with TraPPE showed an average deviation of 15 K between the MS estimated three-phase coexistence line and the experimental one (see Tables IV and V). Despite this shift, the shape of the equilibrium curve is in good agreement with the experimental one. Prediction of three phase coexistence line for TIP4P/2005 and TraPPE shows also the same general slope of the equilibrium curve but 22 K shifted to the left of TIP4P/Ice-TraPPE estimations. This difference of 22 K had already been pointed out by Conde and Vega,[36] who found a correlation between the estimation of T_3 and the estimated melting temperature T_m of Ice I_h for different H_2O models at the same pressure. In fact, the prediction of T_m between TIP4/Ice and TIP4P/2005 differs exactly 22 K[36] at 0.1 MPa. This correlation is due to the fact that experimental three phase coexistence line of hydrates starts at a temperature close to the melting point of I_h Ice.

Fig. 8 shows the prediction of three phase coexistence line for TIP4P/Ice H_2O and MSM, EPM2, and ZD models for CO_2. As can be seen, not major differences were obtained on the T_3 prediction when different parameterizations of the three interaction site model of CO_2 were used (see Table V). The maximum difference between the estimated T_3 values for a given pressure value among these models is around 4 K only. Previously, it had been demonstrated that these models predict similar vapor-liquid equilibria and interfacial properties,[76,77] but their predictions for the fluid-solid equilibria are on the other hand rather different,[78] and greatly dependent of the molecular quadrupole moment resulting from by the point charge distribution in each parameterization. Furthermore, the trend of all curves in Fig. 8 is quite similar. Then, the

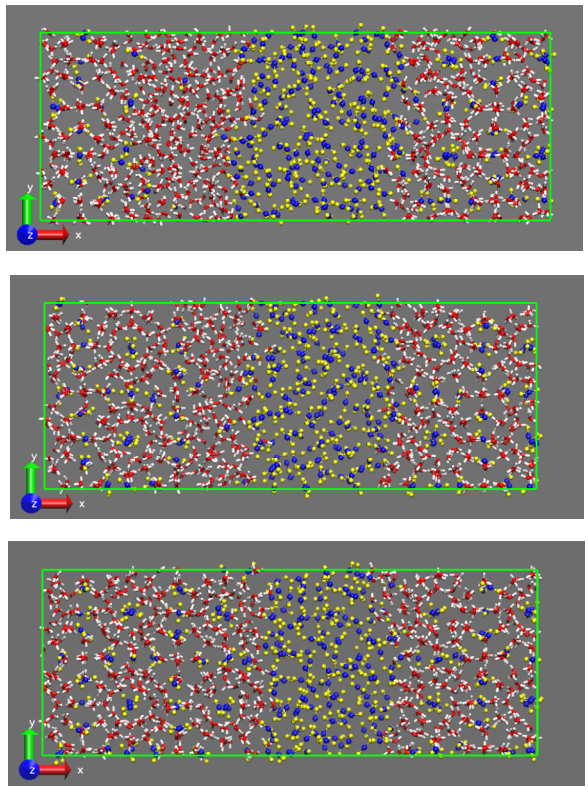

FIG. 6. Snapshots of layer by layer CO_2 hydrate growth, beginning at the interface of liquid H_2O-initial hydrate slab and eventually reaching the hydrate-liquid CO_2 equilibrium.

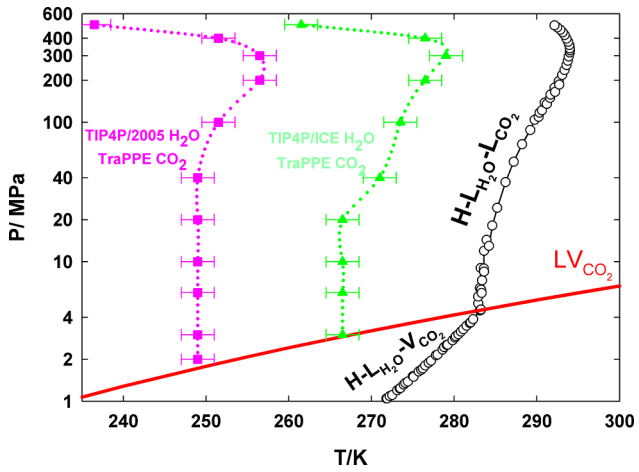

FIG. 7. *PT* projection of the three-phase coexistence line of CO_2 hydrate (hydrate-H_2O-CO_2 calculated using different H_2O molecular models): (pink filled squares) TIP4P/2005 H_2O-TraPPE CO_2, (green filled triangles) TIP4P/Ice H_2O-TraPPE CO_2, (black open circles) experimental data, and (red line) experimental CO_2 vapour pressure curve.

estimation of the hydrate three phase line is greatly dependent on the H_2O molecular model, but the CO_2 model has by far less influence, provided that it meets two conditions: first, the CO_2 vaporization enthalpy is accurately estimated, and then, the original Lorentz Berthelot combination rules are observed. This last condition is so because a tuning on the unlike H_2O-CO_2 interaction parameter may balance the shift from the experimental hydrate coexistence curve, as it is well known and will be discussed in detail later.

The work by Nakano *et al.*[79] shows that CO_2 hydrates exhibit re-entrant behaviour at high pressure. This phenomenon was observed in several hydrates: CH_4,[80] Xe,[81] CO_2,[79] etc. As pressure increases, the hydrate structure shrinks, reducing the size of the hydrate cages. At some temperature and pressure, D cages become too small to fit the guest molecule and stabilize the hydrate structure. Experimental data[79] suggest a maximum temperature of 294 K and 328 MPa on the three coexistence line of CO_2 hydrates. This re-entrant behaviour of CO_2 hydrates has been adequately estimated for the tested H_2O models and all three interaction sites models for CO_2. The results show that the shape of three phase coexistence line obtained by MS is in agreement with the experimental curve at high pressure, and to our knowledge, it is the first time that this phenomenon has been estimated using MS.

Summarizing this section, the combination of TIP4P/Ice with a three interaction site model of CO_2 appears to be the best option for the study of CO_2 hydrate formation. This combination allows predicting the re-entrant phenomena of CO_2 hydrate. Although TIP4P/Ice reproduces accurately the experimental H_2O melting point and the experimental three phase coexistence line of CH_4 hydrates, combined with a LJ model of CH_4, it does not provide a good description of experimental T_3 results combined with a CO_2 model.

C. Optimized potential to predict the three phase coexistence line of CO_2 hydrates

In Sec. III B, it has been shown that the combination of the tested H_2O and CO_2 models were not able to provide a quantitative satisfactory agreement with experimental three phase coexistence line of CO_2 hydrates. Although TIP4P/Ice reproduces experimental melting point of water T_m, it does not reproduce experimental T_3 of CO_2 hydrate combined with a CO_2 model. The relation between T_m and T_3 is clear and had already been demonstrated for CH_4 hydrates[35,36] and CO_2 hydrates (see Sec. III B). Despite the results of this first calculation, there are other alternatives to improve the quantitative results in the estimation of T_3. Let us recall that so far the characteristic parameters of the molecular models were used as originally proposed, without any refit or crossed interaction parameter. The straightforward step would be then considering a cross interaction parameter in the Lorentz-Berthelot rules, with the aim to tune the H_2O-CO_2 interaction.

Following this approach, we have analyzed the changes of T_3 estimation when increasing the strength of the H_2O-CO_2 cross interaction while keeping constant the interaction between identical molecules (Eqs. (1) and (2)). Docherty *et al.*[82] considered also a positive deviation ($\chi = 1.07$) of the crossed interaction parameter to reproduce the excess chemical potential of CH_4 in H_2O for TIP4P/2005 model. This is an effective way to account for the polarization of CH_4 or other molecules in an aqueous solution.[82] This modification succeeded to fix the reported original under prediction of CO_2 adsorption over H_2O interfaces.[77,83] Conde and Vega[35] used the same value ($\chi = 1.07$) to study CH_4 hydrates for TIP4P/2005-H_2O and LJ-CH_4 models, pointing out that the modified cross interaction parameter shifts 5 K the obtained results if compared with the former estimations.

TABLE IV. Cross interaction parameters for the water-CO_2 interaction obtained from Lorentz-Berthelot combining rules ($\chi = 1$) and optimized cross energy interaction ($\chi = 1.13$) to reproduce three phase coexistence line of CO_2 hydrates.

Cross interaction H_2O-CO_2	χ	ϵ_{O-C}/κ_B (K)	ϵ_{O-O}/κ_B (K)	σ_{O-C} (Å)	σ_{O-O} (Å)
TIP4P/Ice-MSM	1	55.470	93.898	2.9759	3.0904
TIP4P/Ice-EPM2	1	54.630	92.422	2.9016	3.0999
TIP4P/Ice-ZD	1	55.321	93.647	2.9793	3.0834
TIP4P/2005-TraPPE	1	50.164	85.807	2.9795	3.0795
TIP4P/Ice-TraPPE	1	53.523	91.553	2.9834	3.1084
TIP4P/Ice-TraPPE	1.13	60.481	103.455	2.9834	3.1084

TABLE V. Three-phase coexistence temperatures (T_3) at different pressures obtained from different combination of H_2O and CO_2 models. The estimated error in T_3 is shown between parentheses. The experimental values were taken from Ref. 1.

P (MPa)	T_3^{simul} (K)	T_3^{simul} (K)	T_3^{simul} (K)	T_3^{simul} (K)	T_3^{simul} (K)	$T_3^{expt.}$ (K)
H_2O	TIP4P/2005	TIP4P/Ice	TIP4P/Ice	TIP4P/Ice	TIP4P/Ice	
CO_2	TraPPE	TraPPE	MSM	EPM2	ZD	
2	249					277.5
3	249(2)	267(2)	269(2)	269(2)	267(2)	280.5
6	249(2)	267(2)	271(2)	269(2)	267(2)	283.2
10	249(2)	267(2)	269(2)	269(2)	269(2)	283.6
20	249(2)	267(2)	271(2)	269(2)	269(2)	284.6
40	249(2)	271(2)	274(2)	274(2)	274(2)	286.2
100	252(2)	274(2)	277(2)	277(2)	277(2)	289.7
200	257(2)	277(2)	282(2)	279(2)	279(2)	293.0
300	257(2)	279(2)	282(2)	277(2)	277(2)	293.9
400	252(2)	277(2)	277(2)	274(2)	269(2)	293.6
500	237(2)	262(2)	262(2)	262(2)	264(2)	292.1

In this case, the objective consists in identifying an optimized χ value to reproduce the experimental data of three phase coexistence line (hydrate-liquid H_2O-liquid CO_2) for CO_2 hydrates. We performed NPT molecular dynamic simulations using TIP4P/Ice H_2O and TraPPe CO_2. TIP4P/Ice reproduces the experimental melting temperature T_m of Ice I_h, and TraPPE model yields the best description of the triple point and melting curve of CO_2.[78] Simulations were performed at the same temperature and pressure conditions and following exactly the same methodology described in Sec. III B. Different cross interaction energy parameter values were tested, until a good compromise was found with $\chi = 1.13$.

Fig. 9 shows the potential energy fluctuations as a function of time for the initial system at 40 MPa and 100 MPa at different temperatures. The general behaviour of the potential energy is similar for the usual Lorentz-Berthelot rules ($\chi = 1$) and for the optimized cross interaction energy ($\chi = 1.13$). The only difference observed is that the time necessary to reach the hydrate-liquid CO_2 equilibrium. The optimized cross interaction energy speeds up around 100 ns the crystallization process because it increases the solubility of CO_2 in H_2O. In

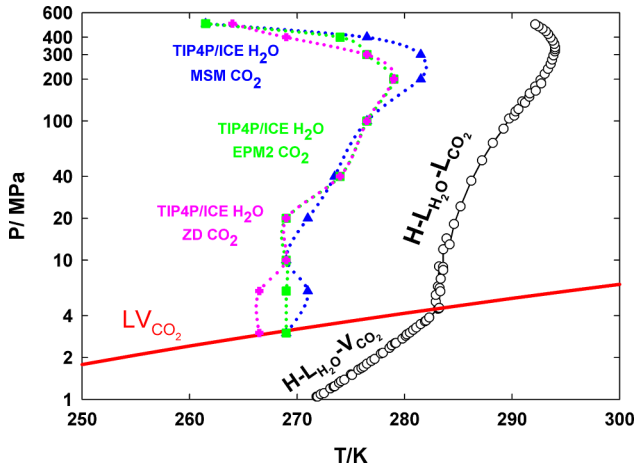

FIG. 8. Representation of the three-phase coexistence temperature T_3 as a function of pressure for several CO_2 models in combination with TIP4P/Ice-H_2O: (blue filled triangles) TIP4P/Ice H_2O-MSM CO_2, (green filled squares) TIP4P/Ice H_2O-EPM2 CO_2, (pink filled crosses) TIP4P/Ice H_2O-ZD CO_2, (black open circles) experimental data, and (red line) experimental CO_2 vapour pressure curve. Error bars, of the same size as those of Figure 7, have been omitted for clarity.

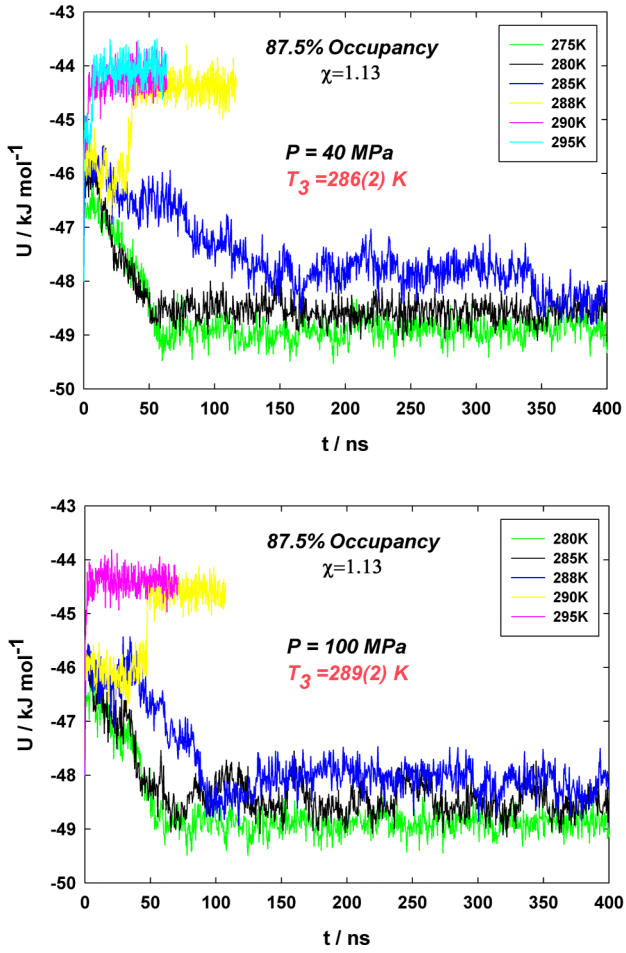

FIG. 9. Evolution of the potential energy of the three phase initial configuration (hydrate-H_2O-CO_2) using the optimized cross energy interaction ($\chi = 1.13$) at (a) 40 and (b) 100 MPa, and temperatures from 275 to 285 K. H_2O was modelled with TIP4P/Ice model, and TraPPE model has been used for CO_2. The cage occupancy of the initial hydrate configuration was 87.5%.

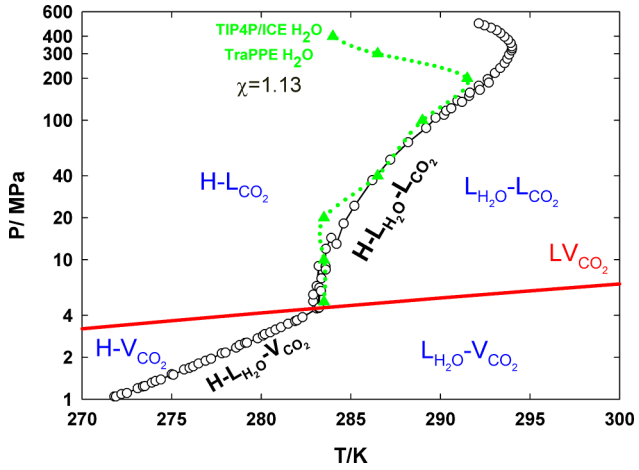

FIG. 10. Estimation of the three-phase coexistence temperature T_3 as a function of pressure for TraPPE CO_2 in combination with TIP4P/Ice H_2O using a positive deviation ($\chi = 1.13$) of the Lorentz-Berthelot combining rules to model the interaction between CO_2 and H_2O: (green filled triangles) TIP4P/Ice H_2O-TraPPE CO_2 ($\chi = 1.13$), (black open circles) experimental data, and (red line) experimental CO_2 vapour pressure curve. Error bars, of the same size as those of Figure 7, have been omitted for clarity.

all cases, the growth of the CO_2 hydrate has also occurred layer by layer and no bubbles were observed. CO_2 hydrate dissociates at 40 MPa for temperatures above 288 K, and the system crystallizes for temperatures below 285 K (see Fig. 9(a)). At 100 MPa, the system crystallizes below 288 K and dissociates below 290 K (see Fig. 9(b)). Therefore, we have obtained $T_3 = 286 \pm 2$ and $T_3 = 289 \pm 2$ K at 40 and 100 MPa, respectively.

The prediction of the complete three phase coexistence line can be seen in Fig. 10 and the values have been presented in Table VI. The combination of TIP4P/Ice H_2O model and the TraPPE-CO_2 model with a positive deviation ($\chi = 1.13$) of the Lorentz-Berthelot combining rules reproduces accurately experimental three phase coexistence line of CO_2 hydrates up to 200 MPa. However, the location of the temperature maximum indicating the re-entrant phenomenon is not predicted correctly. It seems very likely that the increase of cross energy interaction CO_2-H_2O modifies the compressibility of the hydrate structure at very high pressures. In any case, this effect should be analyzed in future works.

TABLE VI. Prediction of the three-phase coexistence line of CO_2 by MS using a positive deviation ($\chi = 1.13$) of the energetic Lorentz-Berthelot combination rule. H_2O was modelled using the TIP4P/Ice model, and TraPPE model has been used to model CO_2. The experimental values were taken from Ref. 1.

P (MPa)	T_3^{simul} (K)	$T_3^{expt.}$ (K)
5	284(2)	282.9
10	284(2)	283.6
20	284(2)	284.6
40	287(2)	286.2
100	289(2)	289.7
200	292(2)	293.0
300	287(2)	293.9
400	284(2)	293.6

Therefore, the combination of TIP4P/Ice model for H_2O and TraPPE model for CO_2 with a positive deviation of Lorentz-Berthelot combining rules turns out to be a good compromise to describe CO_2 hydrates.

The effect of the modification of the χ value on the estimated solubility values of CO_2 in H_2O rich phase along the three phase line has been also estimated from MS results. For the sake of comparison, the correlation from experimental solubility data presented by Diamond and Akinfiev[84] has been used. These authors performed an exhaustive literature review, critically evaluating all published data sets, after which they discarded inconsistent data and offered a correlation for solubility values at pressures up to 100 MPa. Fig. 11 shows the $T - x$ and $P - x$ projections of the estimated CO_2 solubilities, compared with the cited correlation, using both tested χ values. As noted, the $\chi = 1.13$ value doubles CO_2 solubility, thus favouring the migration of these molecules through the aqueous phase towards the hydrate interface, which increases the crystallization rate, but this modification shifts solubility values away from the experimental trend, as shown in these

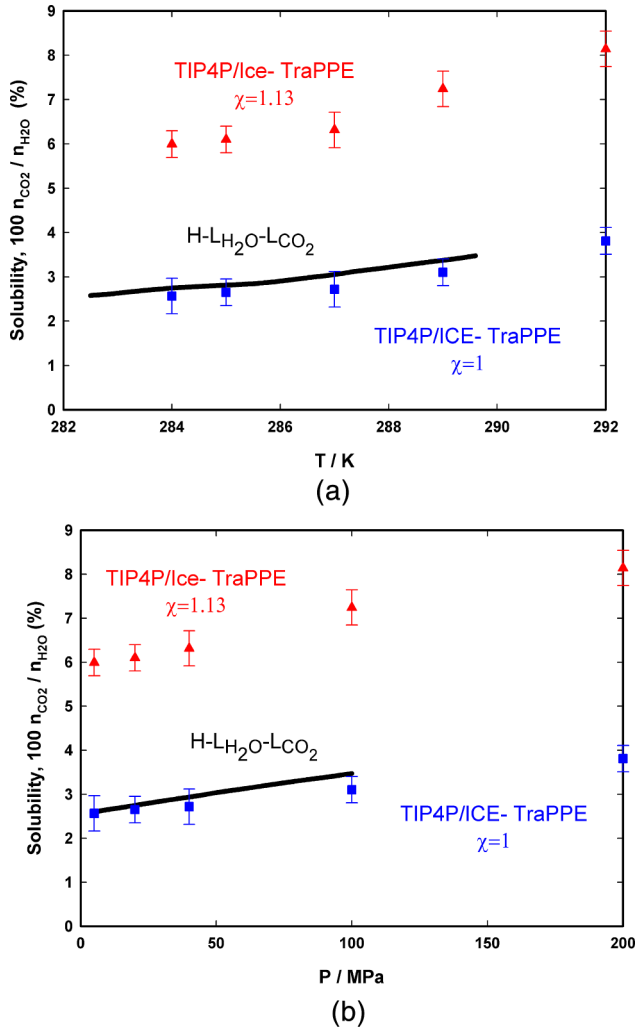

FIG. 11. (a) $T - x$ and (b) $P - x$ projections of the estimated CO_2 solubility values in H_2O, along the three phase line. Solid line represents the experimental correlation by Diamond and Akinfiev,[84] and the symbols are MS results using TIP4P-Ice H_2O and TraPPE CO_2, using Lorentz Berthelot rules with $\chi = 1$ (blue squares) and $\chi = 1.13$ (red triangles).

plots. Only the MS estimated values up to 200 MPa have been shown because there are no experimental solubility values for the high pressure range where the described re-entrant phenomenon occurs, making comparison impossible. On the other coexisting fluid phase, the solubility of H_2O in liquid CO_2 is negligible, as it can be guessed from the density profiles shown in Fig. 5(d), or at least it is not detectable with the number of molecules used in the simulation box used.

IV. CONCLUSIONS

In this work, we have estimated the three phase coexistence line (hydrate-liquid H_2O-liquid CO_2) using molecular dynamics simulations and the direct coexistence method. The initial configuration was composed by three slabs: hydrate, liquid H_2O, and liquid CO_2. Initial CO_2 occupancy in the hydrate slab was varied to determine the role that the specific occupancy of large (T) and small (D) cavities plays on hydrate stability. As a result, we have obtained a clear specific cage occupancy dependence on initial CO_2 hydrate slab in prediction of T_3 and crystallization and dissociation processes. The evolution of the system was the same in all cases where all T cages were initially fully occupied, while leaving empty T cages changed significantly the time evolution of the hydrate slab. The initial value of occupancy of D cages seemed not to be relevant in these calculations.

Then, we have calculated the three phase coexistence line (hydrate-liquid H_2O-liquid CO_2) using TIP4P/2005 and TIP4P/Ice models of H_2O and MSM, EPM2, TraPPE, and ZD models of CO_2 by NPT simulations at 2, 3, 6, 10, 20, 40, 100, 200, 300, 400, and 500 MPa. Initial 87% hydrate slab occupancy was selected to perform this study, as this value approaches reported experimental occupancy data. Results of T_3 for TIP4P/Ice combined with three interaction sites models of CO_2 showed a deviation of 15 K between the estimated and the experimental curves. Despite this temperature shift, the shape of the equilibrium curve is in good agreement with the experimental one. Prediction of three phase coexistence line for TIP4P/2005 is placed 22 K below TIP4P/Ice predictions, and this result is directly correlated with the difference in the estimation of Ice I_h melting temperature T_m between TIP4/Ice and TIP4P/2005, which is exactly 22 K at 0.1 MPa. Although TIP4P/Ice reproduces experimental melting point T_m of Ice I_h, it does not reproduce experimental T_3 of CO_2 hydrate combined with a CO_2 model using Lorentz-Berthelot ideal cross combining rules ($\chi = 1$).

Finally, we have analyzed the modification in the estimation of T_3 when increasing the strength of the H_2O-CO_2 cross interaction while keeping constant alike interactions. The combination of TIP4P/Ice-H_2O and TraPPE-CO_2 with a positive deviation ($\chi = 1.13$) of the Lorentz-Berthelot combining rules reproduces with remarkable accuracy the experimental three phase coexistence line of CO_2 hydrates up to 200 MPa. Nevertheless, the consideration of this nonideal cross energy parameter produces an undesirable loss of accuracy in the estimation of CO_2 solubility in H_2O rich fluid phase.

ACKNOWLEDGMENTS

The authors acknowledge CESGA (www.cesga.es) in Santiago de Compostela, Spain, and MCIA (Mésocentre de Calcul Intensif Aquitain) of the Universités de Bordeaux and Pau et Pays de l'Adour, France, for providing access to computing facilities. Financial support is acknowledged to Ministerio de Economía y Competitividad (Grant Nos. FIS2010-14866 and FIS2012-33621, this one cofinanced with EU FEDER funds, and FIS2013-43209-P), in Spain. J.M.M. acknowledges Fundación Barrié de la Maza (Spain) for a Postdoctroral Grant. Further financial support from Junta de Andalucía, Universidad de Huelva and Carnot Institute (ISIFoR, France) are also acknowledged.

[1]E. D. Sloan and C. Koh, *Clathrate Hydrates of Natural Gases*, 3rd ed. (CRC Press, New York, 2008).
[2]E. D. Sloan, Nature **426**, 353–359 (2003).
[3]R. K. McMullan and G. A. Jeffrey, J. Chem. Phys. **42**, 2725 (1965).
[4]C. W. Mak and R. K. McMullan, J. Chem. Phys. **42**, 2732 (1965).
[5]J. A. Ripmeester, J. S. Tse, C. I. Ratcliffe, and B. M. Powell, Nature **325**, 135 (1987).
[6]K. A. Kvenvolden, Chem. Geol. **71**, 41–51 (1988).
[7]C. A. Koh, A. K. Sum, and E. D. Sloan, J. Nat. Gas Sci. Eng. **8**, 132–138 (2012).
[8]M. D. Max, A. H. Johnson, and W. P. Dillon, *Economic Geology of Natural Gas Hydrate* (Springer, 2006).
[9]*Natural Gas Hydrate in Oceanic and Permafrost Environments*, edited by M. D. Max (Springer, 2011).
[10]R. Boswell, Science **325**, 957–958 (2009).
[11]R. Boswell and T. S. Collett, Energy Environ. Sci. **4**, 1206–1215 (2011).
[12]G. J. Moridis, T. S. Collett, M. Pooladi-Darvish, S. Hancock, C. Santamarina, R. Boswell, T. Kneafsey, J. Rutqvist, M. B. Kowalsky, M. T. Reagan, E. D. Sloan, A. K. Sum, and C. A. Koh, SPE Reservoir Eval. Eng. **14**, 76–112 (2011).
[13]A. K. Sum, C. A. Koh, and E. D. Sloan, Ind. Eng. Chem. Res. **48**, 7457–7465 (2009).
[14]M. Yang, Y. Song, L. Jiang, Y. Zhao, X. Ruan, Y. Zhang, and S. Wang, Appl. Energy **116**, 26–40 (2014).
[15]M. Ricaurte, C. Dicharry, X. Renaud, and J.-P. Torré, Fuel **122**, 206–2017 (2014).
[16]B. Kvamme, A. Graue, T. Buanes, T. Kuznetsova, and G. Ersland, Int. J. Greenhouse Gas Control **1**, 236–246 (2007).
[17]A. K. Sum, D. T. Wu, and K. Yasuoka, MRS Bull. **36**, 205–210 (2011).
[18]B. C. Barnes and A. K. Sum, "Advances in molecular simulations of clathrate hydrates," Curr. Opin. Chem. Eng. **2**, 184–190 (2013).
[19]M. R. Walsh, C. A. Koh, E. D. Sloan, A. K. Sum, and D. T. Wu, Science **326**, 1095 (2009).
[20]Y. Park, D. Kim, J.-W. Lee, D.-G. Huh, K.-P. Park, J. Lee, and H. Lee, Proc. Natl. Acad. Sci. U. S. A. **103**, 12690–12694 (2006).
[21]E. M. Yezdimer, P. T. Cummings, and A. A. Chialvo, J. Phys. Chem. A **106**, 7982–7987 (2002).
[22]P. Dornan, S. Alavi, and T. K. Woo, J. Chem. Phys. **127**, 124510 (2007).
[23]D. Bai, G. Chen, X. Zhang, and W. Wang, Langmuir **28**, 7730–7736 (2012).
[24]D. Bai, X. Zhang, G. Chen, and W. Wang, Energy Environ. Sci. **5**, 7033–7041 (2012).
[25]Y.-T. Tung, L.-J. Chen, Y.-P. Chen, and S.-T. Lin, J. Phys. Chem. B **115**, 15295–15302 (2011).
[26]Y.-T. Tung, L.-J. Chen, Y.-P. Chen, and S.-T. Lin, J. Phys. Chem. C **115**, 7504–7515 (2011).
[27]S. Sarupria and P. G. Debenedetti, J. Phys. Chem. A **115**, 6102–6111 (2011).
[28]A. A. Chialvo, M. Houssa, and P. P. T. Cummings, J. Phys. Chem. B **106**, 442–451 (2002).
[29]R. Sun and Z. Duan, Geochim. Cosmochim. Acta **69**, 4411–4424 (2005).
[30]A. Vidal-Vidal, M. Pérez-Rodríguez, J.-P. Torré, and M. M. Piñeiro, Phys. Chem. Chem. Phys. **17**, 6963–6975 (2015).
[31]S. C. Velaga and B. J. Anderson, J. Phys. Chem. B **118**, 577–589 (2014).
[32]M. M. Conde, C. Vega, C. McBride, E. G. Noya, R. Ramírez, and L. M. Sesé, J. Chem. Phys. **132**, 114503 (2010).
[33]S. J. Wierzchowski and P. A. Monson, Ing. Eng. Chem. Res. **45**, 424–431 (2006).

[34]S. J. Wierzchowski and P. A. Monson, J. Phys. Chem. B **111**, 7274–7282 (2007).
[35]M. M. Conde and C. Vega, J. Chem. Phys. **133**, 064507 (2010).
[36]M. M. Conde and C. Vega, J. Chem. Phys. **138**, 056101 (2013).
[37]V. K. Michalis, J. Costandy, I. N. Tsimpanogiannis, A. K. Stubos, and I. G. Economou, J. Chem. Phys. **142**, 044501 (2015).
[38]L. Jensen, K. Thomsen, N. Von Solms, S. Wierzchowski, M. R. Walsh, C. A. Koh, E. D. Sloan, D. T. Wu, and A. K. Sum, J. Phys. Chem. B **114**, 5775–5782 (2010).
[39]G. S. Smirnov and V. V. Stegailov, J. Chem. Phys. **136**, 044523 (2012).
[40]S. Ravipati and S. N. Punnathanam, Ind. Eng. Chem. Res. **51**, 9419 (2012).
[41]M. Yousuf, S. B. Qadri, D. L. Knies, K. S. Grabowski, R. B. Coffin, and J. W. Pohlman, Appl. Phys. A **78**, 925–939 (2004).
[42]V. Buch, P. Sandler, and J. Sadlej, J. Phys. Chem. B **102**, 8641 (1998).
[43]J. D. Bernal and R. H. Fowler, J. Chem. Phys. **1**, 515 (1933).
[44]D. V. D. Spoel, E. Lindahl, B. Hess, G. Groenhof, A. E. Mark, and H. J. C. Berendsen, J. Comput. Chem. **26**, 1701 (2005).
[45]S. Nosé, J. Chem. Phys. **81**, 511 (1984).
[46]W. G. Hoover, Phys. Rev. A **31**, 1695 (1985).
[47]M. Parrinello and A. Rahman, J. Appl. Phys. **52**, 7182 (1981).
[48]S. Nosé and M. L. Klein, Mol. Phys. **50**, 1055 (1983).
[49]U. Essmann, L. Perera, M. L. Berkowitz, T. Darden, H. Lee, and L. G. Pedersen, J. Chem. Phys. **103**, 8577 (1995).
[50]W. L. Jorgensen, J. Chandrasekhar, J. Madura, R. W. Impey, and M. Klein, J. Chem. Phys. **79**, 926 (1983).
[51]H. J. Berendsen, J. P. M. Postma, W. F. van Gunsteren, and J. Hermans, in *Intermolecular Forces*, edited by B. Pullman (Reidel Publishing, 1981), pp. 331–342.
[52]C. D. Berweger, W. F. V. Gunsteren, and F. Müller-Plathe, Chem. Phys. Lett. **232**, 429 (1995).
[53]H. J. Berendsen, J. R. Grigera, and T. P. Straatsma, J. Phys. Chem. **91**, 6269–6271 (1987).
[54]J. L. F. Abascal and C. Vega, J. Chem. Phys. **123**, 234505 (2005).
[55]J. L. F. Abascal, E. Sanz, R. García Fernández, and C. Vega, J. Chem. Phys. **122**, 234511 (2005).
[56]C. S. Murthy, K. Singer, and I. R. McDonald, Mol. Phys. **44**, 13 (1981).
[57]D. Moller and J. Fischer, Fluid Phase Equilib. **100**, 35 (1994).
[58]C. S. Murthy, S. F. Oshea, and I. R. M. Donald, Mol. Phys. **50**, 531 (1983).
[59]J. G. Harris and K. H. Yung, J. Phys. Chem. **99**, 12021 (1995).
[60]J. J. Potoff and J. I. Siepmann, AIChE J. **47**, 1676 (2001).
[61]Z. Zhang and Z. Duan, J. Chem. Phys. **122**, 214507 (2005).
[62]J. S. Rowlinson and F. L. Swinton, *Liquids and Liquid Mixtures* (Butterworths, London, 1982).
[63]N. J. English, J. K. Johnson, and C. E. Taylor, J. Chem. Phys. **123**, 244503 (2005).
[64]E. M. Myshakin, H. Jiang, R. P. Warzinski, and K. D. Jordan, J. Phys. Chem. A 1913–1921 (2009).
[65]N. J. English and G. M. Phelan, J. Chem. Phys. **131**, 074704 (2009).
[66]S. Alavi and J. A. Ripmeester, J. Chem. Phys. **132**, 144703 (2010).
[67]N. I. Papadimitriou, I. N. Tsimpanogiannis, I. G. Economou, and A. K. Stubos, Mol. Phys. **112**, 2258–2274 (2014).
[68]A. Valtz, A. Chapoy, C. Coquelet, P. Paricaud, and D. Richon, Fluid Phase Equilib. **226**, 333–344 (2004).
[69]J. Vatamanu and P. G. Kusalik, J. Phys. Chem. B **110**, 15896 (2006).
[70]J. Vatamanu and P. G. Kusalik, J. Chem. Phys. **126**, 124703 (2007).
[71]L. C. Jacobson and V. Molinero, J. Phys. Chem. B **114**, 7302 (2010).
[72]M. Uddin and D. Coombe, J. Phys. Chem. A **118**, 1971–1988 (2014).
[73]T. Uchida, Waste Manage. **17**, 343 (1997).
[74]S. Circone, L. A. Stern, S. H. Kirby, W. B. Durham, B. C. Chakoumakos, C. J. Rawn, A. J. Rondinone, and Y. Ishii, J. Phys. Chem. B **107**, 5529–5539 (2003).
[75]J. R. Espinosa, E. Sanz, C. Valeriani, and C. Vega, J. Chem. Phys. **139**, 144502 (2013).
[76]J. M. Míguez, M. M. Piñeiro, and F. J. Blas, J. Chem. Phys. **138**, 034707 (2013).
[77]J. M. Míguez, J. M. Garrido, F. J. Blas, H. Segura, A. Mejía, and M. M. Piñeiro, J. Phys. Chem. C **118**, 24504–24519 (2014).
[78]G. Peréz-Sánchez, D. González-Salgado, M. M. Piñeiro, and C. Vega, J. Chem. Phys. **138**, 084506 (2013).
[79]S. Nakano, M. Moritoki, and K. Ohgaki, J. Chem. Eng. Data **43**, 807–810 (1998).
[80]U. A. Dyadin, E. Y. Aladko, and E. G. Larionov, Mendeleev Commun. **7**, 34–35 (1997).
[81]U. A. Dyadin, E. G. Larionov, D. S. Mirinskij, T. V. Mikina, E. Y. Aladko, and L. I. Starostina, J. Inclusion Phenom. Mol. Recognit. Chem. **28**, 271–285 (1997).
[82]H. Docherty, A. Galindo, C. Vega, and E. Sanz, J. Chem. Phys. **125**, 074510 (2006).
[83]C. Miqueu, J. M. Míguez, M. M. Piñeiro, T. Lafitte, and B. Mendiboure, J. Phys. Chem. B **115**, 9618–9625 (2011).
[84]L. W. Diamond and N. N. Akinfiev, Fluid Phase Equilib. **208**, 265–290 (2003).